Structural and Optical Response of Polymer-Stabilized Blue Phase Liquid Crystal Films to Volatile Organic Compounds

Yu Yang[a,b], Young-Ki Kim[†,a], Xin Wang[a], Michael Tsuei[a], Nicholas L. Abbott[,a]*

a Smith School of Chemical and Biomolecular Engineering, Cornell University, Ithaca, USA

b Department of Chemical and Biological Engineering, University of Wisconsin–Madison, USA

Keywords: liquid crystal; blue phase; polymer network, volatile organic compound; optical and structural response; sensor;

Abstract

Engineering useful mechanical properties into stimuli-responsive soft materials without compromising their responsiveness is, in many cases, an unresolved challenge. For example, polymer networks formed within blue phase liquid crystals (BPs) have been shown to form mechanically robust films, but the impact of polymer networks on the response of these soft materials to chemical stimuli has not been explored. Here we report on the response of polymer stabilized BPs (PSBPs) to volatile organic compounds (VOCs, using toluene as a model compound), and compare the response to BPs without polymer-stabilization and to polymerized nematic and cholesteric phases. We find that PSBPs generate an optical response to toluene vapor (change in reflection intensity under crossed polars) that is six-fold greater in sensitivity than the polymerized nematic or cholesteric phases, and with a limit of detection (140 ± 10 ppm at 25 °C) that is relevant to measurement of permissible exposure limits for humans. Additionally, when compared to BPs that have not been polymerized, PSBPs respond to a broader range of toluene vapor concentrations (5000 ppm versus <1000 ppm) over a wider temperature interval (25 °C to 45 °C versus 45 °C to 53 °C). We place these experimental observations into the context of a simple thermodynamic model to explore how the PSBP response reflects the effect of toluene on competing contributions of double twisted LC

cylinders, disclinations and polymer network to the free energy that controls the PSBP lattice spacing. Overall, we conclude that the mechanical and thermal stability of PSBPs, when combined with their optical responsiveness to toluene, make this class of self-supporting LCs a promising one as the basis of passive and compact (e.g., wearable) sensors for VOCs.

Introduction

Liquid crystals (LCs) are phases that possess both fluid-like mobility of liquids and long-range ordering characteristic of crystalline solids,[1] a combination of properties that allows localized molecular-level events to be amplified into macroscopic ordering transitions that are easily visualized due to the optical properties of LCs.[2] These attributes have motivated a wide range of past studies of the responses of LCs to external stimuli, including electric fields,[3-4] shear stresses,[5] hazardous gases,[6-9] and biological molecules.[10-12] For example, surface-driven orientational transitions (and thus optical responses) of LCs have been triggered by reactive gases that interrupt metal ion-ligand coordination[6-8] or acid-base interactions of LCs at interfaces.[9] Past efforts to detect volatile organic compounds (VOCs) with LCs, however, have met with limited success largely because most VOCs do not possess reactive functional groups.[13-20]

The development of materials that indicate human exposure to VOCs have the potential to be useful in a range of contexts, including industrial, commercial and home settings.[21] Exposure to toluene, for instance, is limited to 200 ppm, time-averaged over 8-hours, by the Occupational Safety and Health Administration (OSHA).[22] Most VOCs, however, cannot be detected using methods (e.g., electrochemical detectors)[23] commonly employed to validate human exposure limits for reactive/electroactive species. Additionally, methods based on infrared spectroscopy[24] and metal oxide semiconductor detectors[25] are not suitable as the basis of wearable sensors. LCs, due to their compactness, simplicity and passive response, represent a potentially useful approach for measurement of personal exposure to VOCs if they can be prepared in ways that combine thermal and mechanical stability along with sensitivity to the VOCs.[13-20] In one previously reported approach,[14-15] the presence of VOCs was marked by the observation of a decrease in the clearing point (i.e., nematic-to-isotropic transition temperature) of a nematic LC. To achieve a response to 100 ppm of p-xylene, however, it was necessary to heat the LC to within ~0.5 °C[14] of the clearing point,[15] a requirement that makes implementation of the approach impractical for personal monitoring.

Chiral LCs have been explored as the basis of materials that respond to low concentrations of VOCs[16-19] because molecular-level changes can be amplified by supramolecular organization of the LC (i.e., twist of LC) induced by the chirality.[26-27] In a cholesteric (i.e., chiral nematic) phase, the LC director undergoes a helical twist, with a period of rotation of 2π over a distance known as the pitch. Prior studies have reported an increase in the helical pitch of cholesteric mixtures of nematic E7 and chiral dopants, when the LC was exposed to either acetone or toluene vapor.[17] By analyzing the spectrum of reflected light, they reported detection of gas phase concentrations of toluene as low as 48 ppm. In this paper, for reasons stated below, we move beyond cholesteric phases to investigate the response of an additional class of chiral LCs, so-called blue phase (BP) LCs (named for the blue color they exhibited when initially discovered).[28]

BPs appear as intermediate phases near the cholesteric-to-isotropic transition temperature when high concentrations of chiral dopants are dissolved into a nematic LC. The presence of the high chiral dopant concentration leads to formation of so-called double twist cylinders (DTCs,

Figure 1a) of LC that assemble into three-dimensional lattices.[1, 29] For example, BPI (Figure 1b) and BPII (Figure 1c) possess body center cubic (BCC) and simple cubic (SC) structures, respectively. The DTCs in BPs are energetically favored over single twist cylinders formed in cholesteric phases,[1, 30] but DTCs cannot fill space continuously, and topological line defects form between the DTCs. Past studies[31] have revealed that BPs form via a delicate balance of energetic contributions arising from both the DTCs and disclinations (or defect lines, dark blue lines in Figure 1d and e) and that this energetic competition restricts formation of BPs to a narrow temperature interval below the clearing point. The three-dimensional periodicity of the BPs leads to Bragg diffraction in the visible part of the light spectrum.

Our focus on BPs, as reported in this paper, was motivated by the proposal that BPs, because they arise from a delicate balance of competing energetic contributions (as discussed above), may provide a sensitive response to VOCs. This proposal receives support from prior studies that have shown than subtle stimuli, including biological adsorbates,[32] electric fields,[33-34] and mechanical strain,[35] can trigger a change in BP structure and thus Bragg diffraction (providing a convenient means to transduce the stimuli). Additionally, a recent study demonstrated that toluene vapor can trigger cholesteric phases to transform to BPs.[36] This prior study, however, also highlights a key limitation of BPs noted above, namely their existence within only a narrow temperature interval (typically 1–3 °C) below the clearing point. The narrow temperature interval limits the potential utility of BPs as a material to report the presence of VOCs.

In this paper, we explore the use of polymerization to thermally and mechanically stabilize BPs in the presence of VOCs. Our approach builds from prior efforts that have investigated several methods for stabilization of BPs in optical devices, including polymerization of BPs,[33, 37] addition of nanoparticles,[38-39] and synthesis of dimeric[34] or bent-core[40] mesogens. Polymerization, in particular, has been reported to stabilize BPs over temperature intervals of more than 60 K.[33] Additionally, and of relevance to development of wearable sensors for personal monitoring, polymer networks provide mechanical properties that enable the preparation of self-supporting films[35] that can facilitate integration into wearable devices. We compare the response of PSBPs to toluene vapor to BPs prior to polymerization and to polymerized nematic and cholesteric phases. Our work reveals three key findings. First, our work demonstrates that PSBPs are more sensitive reporters of VOCs than polymerized cholesteric phases or polymerized nematic phases. Specifically, the differential optical response of the PSBP was found to be six-fold greater than that of polymerized cholesteric and nematic LCs when compared at the same concentration of toluene vapor. Second, our study reveals that the presence of the polymer network within the PSBP generates a response to VOCs that occurs over a broader concentration range relative to BPs that have not been stabilized by polymer networks. Third, we place our experimental measurements within the context of a simple thermodynamic model to reveal how the PSBP response reflects the effect of toluene on the competing contributions of double twisted LC cylinders, disclinations and the polymer network to the free energy that controls the PSBP lattice spacing.

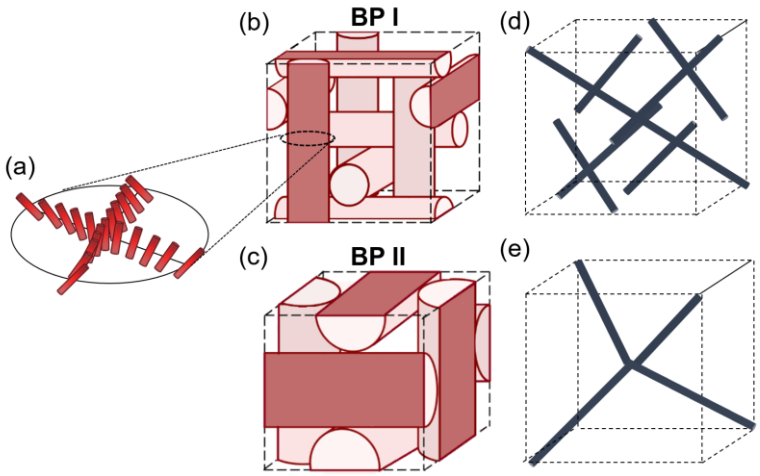

Figure 1. a-e) Schematic illustrations of BP structure, showing (a) director alignment in the cross-section of a double twist cylinder (DTC), (b) DTC configuration and (d) corresponding lattice of disclinations in BPI, and (c) DTC configuration and (e) corresponding lattice of disclinations in BPII.

Materials and Methods

Materials

The nematic LC HTW45800-000 (HTW) and the chiral dopant 4-(1-methylheptyloxycarbonyl)phenyl-4-hexyloxybenzoate (S-811) were purchased from Hecheng Display Technology Co.,Ltd. The monomer 2-methyl-1,4-phenylenebis(4-(3-(acryloyloxy)propoxy)benzoate) (RM257) was purchased from BOC Sciences. Trimethylolpropane triacrylate (TMPTA), 2,2-dimethoxy-2-phenylacetophenone (DMPAP) and toluene (99.5% purity) were purchased from Sigma-Aldrich (St. Louis, MO). Fisher Finest Premium Grade glass slides were obtained from Fisher Scientific (Pittsburgh, PA). Copper 75 mesh TEM grids were purchased from Electron Microscopy Sciences. Polyimide 2555 was purchased from HD Microsystems.

Preparation of LC/monomer mixture

The LC/ monomer premixture composed of 46.6 wt% HTW, 32.4 wt% S811, 18.2 wt% RM257, 0.8 wt% TMPTA and 2.0 wt% DMPAP were prepared by vortexing for 10 min at 3000 rpm. To obtain a homogeneous mixture, we heated the mixture to form an isotropic phase. We note that the choice of mixture composition was guided by previous reports.[37]

Preparation of optical cells

Optical cells were assembled by spacing apart two bare glass slides or polyimide-coated glass slides using 20 µm thick plastic film spacers. Polyimide-coated glass slides were prepared by spin-coating Polyimide 2555 solution onto the slides using a Laurell spin coater, baking the slides at 250 °C and then rubbing the surfaces unidirectionally with fabric. The optical cells prepared from polyimide-coated glass slides were used for characterization of the lattice spacing and measuring the Kossel diagram of BPs.

Synthesis of PSBP films

The premixture described above was injected into an optical cell as an isotropic phase heated to 60 °C using a hotstage (Linkam, TMS 94). The polymerization process was performed as follows: first, the sample was cooled to form the BP II (47 °C) and polymerized using UV-light that illuminated the top surface of the optical cell (1.8 mW/cm^2, 365 nm) for 2 s; second, the sample was cooled from 47 °C to 43 °C and polymerized for an additional 3 s; finally, the sample was cooled to 35 °C and polymerized for 30 min. A cooling rate of 1 °C /min was used during these steps. We cooled the sample during the polymerization process to keep the system in the BPII state (as the polymerization reaction proceeds, the change in composition of the system results in a decrease in the BPII-to-isotropic phase transition temperature). Before exposure to toluene vapor, the bottom substrate of the optical cell was detached from the PSBP film with a razor blade and half of the film was covered with cover glass to prevent exposure to toluene vapor.

Synthesis of polymerized cholesteric and polymerized nematic films

Polymerized cholesteric phases were prepared using the same mixture used to prepare the PSBP. The polymerized nematic phase was prepared using 79.0 wt% HTW, 18.2 wt% RM257, 0.8 wt% TMPTA and 2.0 wt% DMPAP. The polymerization of both films was performed at 25 °C for 30 min, using procedures similar to those described above for preparation of PSBP.

Exposure system

We used two exposure systems in the experiments reported in this manuscript. System 1 was operated under partial vacuum and was used to measure the response of the PSBP as a function of toluene concentration. A detailed description of this exposure system can be found in a prior study.[13] Briefly, the PSBP sample was placed in a vacuum chamber and toluene vapor was introduced to a predetermined vapor pressure. The film was equilibrated with the toluene vapor for 2–3 min before characterization. To enable comparison between data sets obtained in the two exposure systems used in our study, we convert the partial pressure of toluene vapor measured in System 1 to its corresponding concentration in parts-per-million units if present in air at 1atm (see ref 13 for details).

System 2 was operated at atmospheric pressure and was used to expose samples to a constant concentration of toluene vapor for a prolonged period (see Figure S1 in Supporting Information (SI) for a schematic illustration of the experimental setup). System 2 comprised three parts. First, toluene vapor was generated by flowing N_2 gas through liquid toluene cooled by an ice/water mixture. The toluene was cooled to lower the saturated vapor pressure. Second, the N_2 stream saturated with toluene vapor was heated back to room temperature and then further diluted by mixing with an additional N_2 stream to obtain the desired concentration of toluene vapor. Third, the diluted toluene/N_2 stream was fed into a chamber containing the polymerized LC films. The exposure system was home-built using stainless steel tubing and connections. The temperature in the chamber was controlled using a coil heater, and measured with a thermocouple.

Optical Microscopy

Optical images of the samples were obtained under reflection mode (using white light illumination; crossed polars; normal incidence) using an optical microscope (Olympus America Inc. (Melville, NY)). Image intensity was analyzed using ImageJ software.

Lattice spacing characterization

The reflectance spectra of the PSBP films were measured using a reflectometer (Filmetrics, Inc.), as detailed in SI.

Safety considerations

Toluene can cause symptoms such as headaches, dizziness, cracked skin and irritated eyes.[22] All experiments involving toluene, including generation of a vapor from liquid toluene and exposure of LC samples to toluene vapor, were performed in a fumehood with personal protective equipment worn.

Results

Preparation of polymerized BP, cholesteric and nematic LC films

We prepared PSBP films by *in situ* photopolymerization of a mixture comprising HTW (which exhibits a nematic LC phase from −30 °C to 101 °C), the bifunctional monomer RM257 (Figure 2a), the chiral dopant S811 (Figure 2b), the crosslinker TMPTA (Figure 2c) and a photoinitiator (DMPAP). The mixture, heated to form an isotropic phase, was confined between two glass substrates separated by 20 μm-thick spacers. Subsequently, the sample was cooled to form BPII and then polymerized under UV-light (1.8 mW/cm^2, 365 nm) (see **Materials and Methods**). We note that PSBP films prepared from mixtures comprising >10 wt% bifunctional monomer are sufficiently stable mechanically[35] to permit removal of the bottom substrate, which enabled exposure of one face of the PSBP film to toluene vapor.

The phase diagram of the BP mixture, measured before and after polymerization, is shown in Figure 2d. The phase behavior was determined by heating the samples on an optical microscope in reflection mode (crossed polars; Figure S2, SI). Before polymerization, the LC mixture exhibited BP I and BP II phases between 45 °C and 53 °C. In contrast to past studies that performed polymerization of BPI phases,[41-42] as noted above, we polymerized the BPII phase as the temperature interval over which BPII is stable (~7 °C) is wider (thus requiring less precise temperature control) than BPI (~1 °C). After polymerization, the temperature interval over which BPII was observed to be stable increased from ~7 °C to more than 35 °C (Figure 2d). We confirmed that the stabilized phase was BPII by polymerizing the mixture in a polyimide-coated optical cell (planar anchoring of the LC) that aligned the BP lattice. The Kossel diagram (see SI for information regarding measurement and interpretation) of the PSBP (Figure 2e, circular pattern) is consistent with the (100) plane of BPII.[43-44] Additional evidence that the PSBP has the BPII phase structure is presented below.

Polymerized cholesteric films were prepared using the same mixture composition as used above to form the PSBP but with the polymerization performed in the cholesteric phase at 25 °C. The polymerized nematic phase was prepared by omitting the chiral dopant (clearing point of the mixture was 104 ± 1 °C) and performing the polymerization at 25 °C.[45] Both the polymerized cholesteric and polymerized nematic phases were stable over temperature intervals larger than 35 °C (Figure 2d).

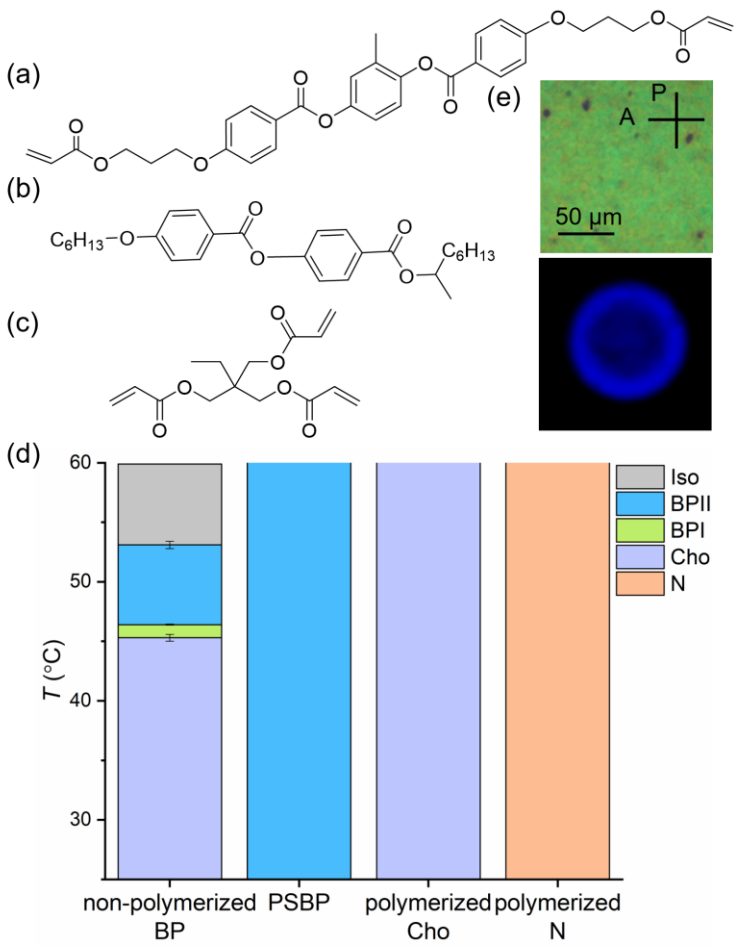

Figure 2. (a-c) Molecular structures of a) RM257, b) S811 and c) TMPTA; (d) Phase diagram of BP LC mixture before (non-polymerized BP) and after polymerization (PSBP), polymerized cholesteric (Cho), and polymerized nematic (N). Data are based on three independent samples. Error bars are standard deviations. (e) Optical micrograph of a PSBP film (crossed polars, reflection mode) and its corresponding Kossel diagram.

Response of PSBP to toluene vapor, and comparision to polymerized cholesteric and nematic LCs

We exposed the polymerized LC films (BP, cholesteric, nematic) to toluene vapor and compared their differential optical responses (see **Materials and Methods**). These experiments were performed using the approach depicted in Figure 3a: one half of each polymerized LC film (region (i) in Figure 3a) was exposed to toluene vapor while the other half of the polymerized film (region (ii) in Figure 3a) was masked by cover glass to prevent toluene exposure (i.e., to serve as a reference). The polymerized samples were placed in a chamber through which we flowed in sequence N_2 gas (t = 0 min to 4.5 min), toluene vapor (t = 4.5 min to 14.5 min; 930 ± 70 ppm) and then N_2 gas at 25 °C (t > 14.5 min). To minimize the influence of factors such as fluctuations in temperature on the optical response, we report the differential optical response of

each polymerized film (measured using white light; crossed polars; normal incidence) as the difference between the image intensities (R) of reflectance micrographs obtained from regions (i) and (ii) (see Figure 3a) at exposure times 0 and t, which we express as $\Delta R = \Delta R(\text{i}) - \Delta R(\text{ii})$ (Figure 3b). In addition, below we use the term sensitivity to indicate the magnitude of the change in the response signal to a given change in VOC concentration, and limit of detection to indicate the lowest concentration at which the signal-to-noise ratio is 10:1 (where noise is calculated as the standard deviation of the baseline signal value).

Inspection of Figure 3b reveals that ΔR of the polymerized cholesteric LC initially inreased upon exposure to toluene vapor ($\Delta R = 0.8 \pm 0.2$) and then subsequently decreased slightly to a steady state response ($\Delta R = 0.6 \pm 0.2$). In contrast, the reflectivity of both the PSBP and polymerized nematic monotonically decreased upon exposure to toluene vapor. Interestingly, the partial decrease in ΔR after the initial rise of the cholesteric response has a dynamic and magnitude that is comparable to the nematic LC, suggesting that it may reflect a toluene-induced change in local order of both polymerized LCs. After the initial change, the value of ΔR for each polymer film was measured to be invariant between $t = 8 \sim 14$ min, consistent with the LC films having equilibrated with the toluence vapor within 3 min. The similarity of equilibration time across all three types of polymer films suggests that it is likely determined by a common mechanism, such as diffusion of toluene across the films. However, we also observed important differences in the initial dynamic response of the three LC films and the magnitudes of response. Specifically, we observed that the time-taken to achieve 66% of the full differential optical response was substantially shorter for the polymerized BP (1.3 ± 0.2 min) and polymerized cholesteric films (0.3 ± 0.2 min) as compare to the polymerized nematic films (2.6 ± 0.8 min). Additionally, inspection of Figure 3c reveals that the magnitudes of ΔR of the PSBP (-4.2 ± 0.4) and polymerized cholesteric LC film (0.6 ± 0.2) are significantly greater than the polymerized nematic LC (-0.3 ± 0.1). We interpret these results to suggest that the large-scale supramolecular organization of the polymerized BP (lattice) and polymerized cholesteric (pitch) LCs generated a rapid and amplified optical response relative to that obtained from the change in orientational order of the polymerized achiral nematic film.

At $t = 15$ min, following the reintroduction of toluene-free N_2 gas into the sample chamber, we measured ΔR of each polymerized LC film return to its initial value, which we interpret to indicate that toluene was stripped from the polymerized LC films and removed by the N_2 flow. Overall, from these results, we conclude that the response of the PSBP to toluene vapor is a reversible process, and that the magnitude of the optical response of the PSBP is larger than either the polymerized nematic or polymerized cholesteric films. Below we discuss the origins of the large optical response and high senstivity of the PSBP to toluene vapor.

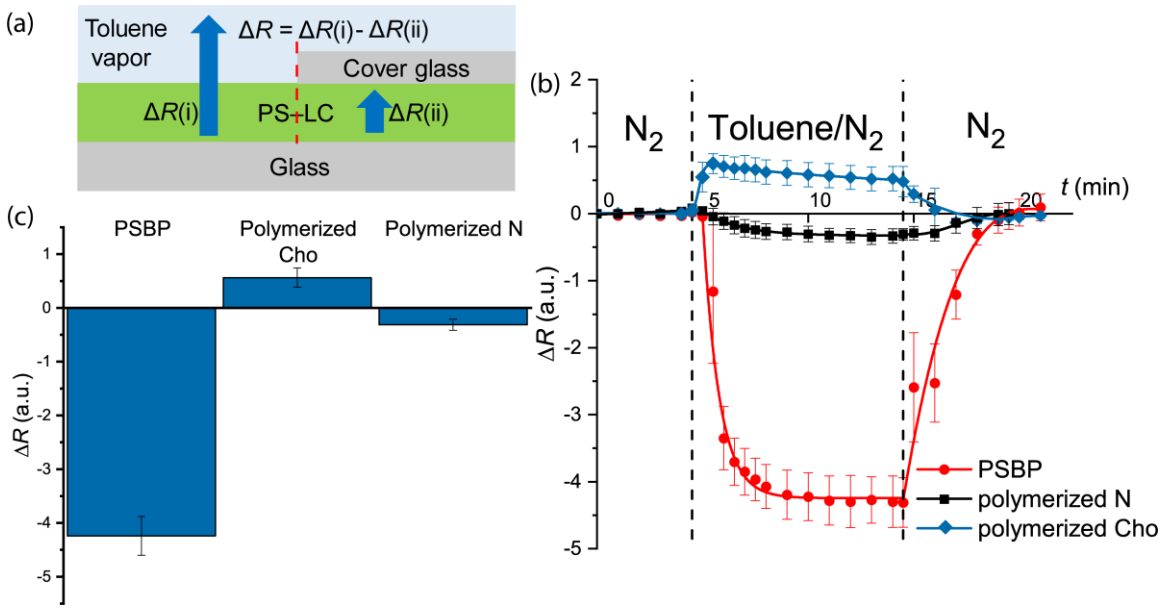

Figure 3. (a) Schematic illustration (side view) of samples used to measure the differential optical response of polymerized LC films to toluene vapor. (b) Measured differential optical signal (ΔR) from PSBP, polymerized cholesteric and polymerized nematic LC films as a function of time (t) during which the films were exposed to toluene vapor (930 ± 70 ppm) at 25 °C and atmospheric pressure. Toluene vapor was present from t = 4.5 min to 14.5 min. (c) Comparison of steady-state differential optical response of polymerized BP, polymerized cholesteric and polymerized nematic LC films. The values of ΔR were averaged between t = 8 ~ 14 min for four independent samples for each type of polymerized LC film. Error bars are standard deviations.

Response of the PSBP as a function of toluene concentrations

Next, we measured the differential optical response of the PSBP as a function of toluene concentration (at 25 °C), with the goal of providing insight into the origins of the large optical response shown in Figure 3. Figure 4a shows the dependence of ΔR on toluene concentration (C). Inspection of Figure 4a reveals ΔR to increase in magnitude with toluene concentration, ending with a phase transition from a polymerized BP to an isotropic phase. We measured the BP to isotropic phase transition of the polymerized samples to occur at a toluene concentration of 5155 ± 60 ppm. Due to the residual birefringence of the polymer network,[46] the micrograph is not completely dark following the phase transition (see micrograph corresponding to 6056 ppm in Figure 4b). In addition, the absence of change in the optical response signal following the LC-to-isotropic phase transition indicates that the optical response arises from the presence of the LC rather than the polymer network. We also found that the PSBP films provided a limit of detection ($\Delta R = -1.1 \pm 0.1$) of C = 140 ± 10 ppm (Figure S3, SI), suggesting that the optical response of the PSBP films is sufficiently sensitive to permit measurement of exposure levels relevant to OSHA requirements (200 ppm for 8-hour time weighted average).[22]

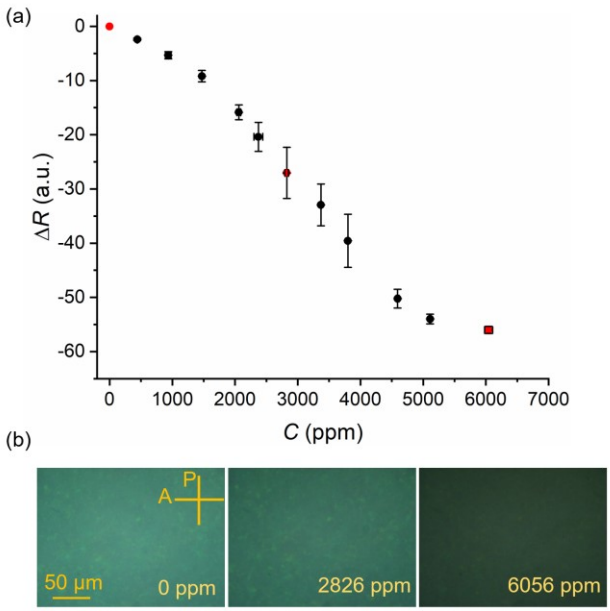

Figure 4. (a) Differential optical response (ΔR) of PSBP films as a function of toluene vapor concentration (C) at 25 °C and atmospheric pressure. (b) Optical reflection micrographs (crossed polars) of PSBP films at C = 0, 2826, and 6056 ppm of toluene vapor (red points in (a)). The data in (a) are based on three independent samples. Error bars are standard deviations.

We hypothesized that the optical response of the PSBP to toluene vapor arises from a change in the BP lattice spacing, since the intensity of Bragg reflected light from PSBPs depends on the lattice spacing.[47] We explored this proposal by measuring the lattice spacing of the PSBP as a function of toluene concentration. The lattice spacing of the PSBP is directly related to the reflection wavelength by the Bragg reflection rule,[48] expressed as

$$\lambda_{hkl} = \frac{2na}{\sqrt{h^2 + k^2 + l^2}} \quad (1)$$

where λ is the peak wavelength of the reflectance spectrum, a is the lattice spacing, n is the refractive index of the BP mixture and h, k, l are Miller indices of the reflection planes. To determine how the lattice spacing of the BP varies with toluene concentration, we characterized the reflectance spectrum of the PSBP film. Figure 5 shows that an increase in toluene concentration causes the peak of the reflectance spectrum to red-shift from λ = 569 nm (at 0 ppm) to λ = 592 nm (at 3668 ppm). This indicates that the PSBP lattice spacing increases with toluene concentration. At the limiting toluene concentration of 5151 ppm, no peak is evident in the reflection spectrum, consistent with results in Figure 4 showing that the PSBP transitioned into an isotropic phase at the highest toluene concentrations. Furthermore, we determined that the reflection peak seen in Figure 5 comes from the (100) plane of the polymerized BPII (Figure S4, SI). Overall, these observations emphasize that the large change in the PSBP reflectance intensity upon exposure to toluene vapor (Figure 3) arises from toluene-induced changes in the

lattice spacing. We return to this point below to discuss the origins of the change in lattice spacing.

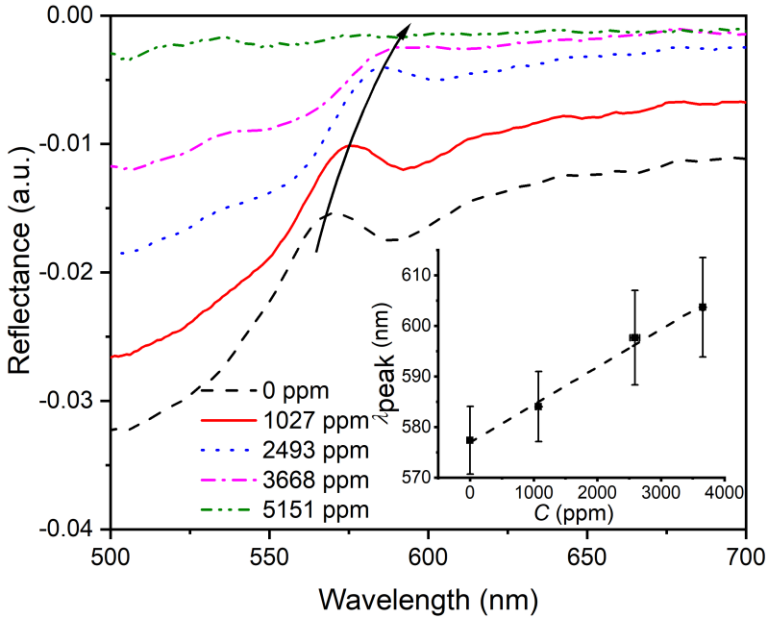

Figure 5. Reflectance spectra of PSBP films as a function of toluene vapor concentration (C = 0, 1027, 2493, 3668, and 5151 ppm) at 25 °C and atmospheric pressure. The arrow indicates the peak reflectance, and the insert shows the relationship between wavelength at peak reflectance (λ_{peak}) and toluene vapor concentration (C). The data in the insert are based on three independent samples. Error bars are standard deviations.

The effect of polymer networks on the response of PSBP to toluene

Kikuchi *et al.*[33] proposed that BPs are stabilized by polymerization because the polymer networks localize in the disclinations of the phase. To understand the effect of the polymer network of a polymerized BP on the response to toluene vapor, we compared the change in lattice spacing of PSBPs to BPs that were not polymerized. As described above, the lattice spacing was calculated from reflectance data (Figure 5 and Figure S5, SI) according to the Bragg reflection rule. From the plots in Figure 6a, which show the relationship between the change of lattice spacing (Δd) and toluene concentration before and after polymerization, we make two key observations.

First, the concentrations of toluene vapor that trigger the initial responses of the PSBP and BP (not polymerized) are different. For the PSBP, the BPII structure was stable at room temperature and exposure to toluene vapor led to a continuous increase in lattice spacing from 140 ± 10 ppm up to a toluene concentration of 3110 ± 81 ppm. In contrast, in the absence of polymerization, the cholesteric phase was stable at room temperature and a threshold concentration of toluene vapor (5236 ± 26 ppm) was required to induce the phase transition from the cholesteric to BPII at room temperature.

Second, the rate of change of the lattice spacing as a function of toluene concentration was measured to differ for PSBP and BP (not polymerized). Specifically, we found the rate of expansion of the lattice spacing of the PSBP (0.003 nm/ppm) to be three times lower than that before polymerization (0.01 nm/ppm). Although the sensitivity of the BP prior to polymerization is higher than the PSBP, the BP prior to polymerization responds over a relatively narrow range of concentrations, thus the PSBP provides a larger dynamic range for quantification of toluene exposure. We note that the lowering of sensitivity caused by polymerization of the BP does not prevent the PSBP from providing a response that is sufficient to meet the requirements of OSHA (200 ppm for 8-hour time weighted average). We propose that potential causes of the decrease in sensitivity caused by polymerization of the BP include: (i) that the disclination cores of the BP are occupied by the polymer network, and thus the free energy of the BP is less readily perturbed by the partitioning of toluene into defect cores and/or (ii) that the polymer network within the BP acts as a mechanical constraint on the PSBP lattice expansion. Both factors also potentially contribute to prior observations that the temperature-dependence of the lattice spacing of a BP is lowered by polymerization.[49]

We found that polymerization of the BP not only increased the concentration range over which the BP responds to toluene but that it also broadened the temperature range over which toluene can be measured. Figure 6b shows the response of the PSBP to 400 ± 60 ppm of toluene at T = 25, 35, 40, and 45 °C. In contrast, when using BPs that were not polymerized, toluene could not be detected below 45 °C, and could only be detected over a ~8 °C temperature interval above 45 °C (45 °C to 53 °C).[36] Inspection of Figure 6b also shows that the sensitivity of the PSBP to toluene vapor increases (magnitude of ΔR increases from 2.2 ± 0.1 to 4.6 ± 0.3) with temperature (from 25 °C to 45 °C). We hypothesize that two factors contribute to this increase: (i) the temperature-dependence of the lattice spacing and/or (ii) a higher solubility of toluene in the LC at higher temperature. Here we address the temperature-dependence of the solubility of toluene in the LC and return to consider the temperature-dependence of the lattice spacing in the Discussion. Past studies have reported that the solubilities of N_2, CO_2 and Ar in LCs increase weakly with temperature.[50] Assuming the temperature dependence of the solubility of toluene in our study to be similar to that of CO_2 in MBBA (N-(4-methoxybenzylidene)-4-butylaniline, a compound that forms a room temperature nematic phase),[50] we estimate the solubility of toluene to increase by a factor of 1.8 with temperature from 25 °C to 40 °C. This leads us to predict that the response of the PSBP to 400 ppm toluene at 40 °C will be similar to 720 ppm of toluene at 25 °C, a prediction that is consistent with our experimental observations (−3.5 ± 0.3 for 720 ppm of toluene at 25 °C (Figure S3, SI) versus −3.8 ± 0.6 for 400 ppm toluene at 40 °C (Figure 6b)).

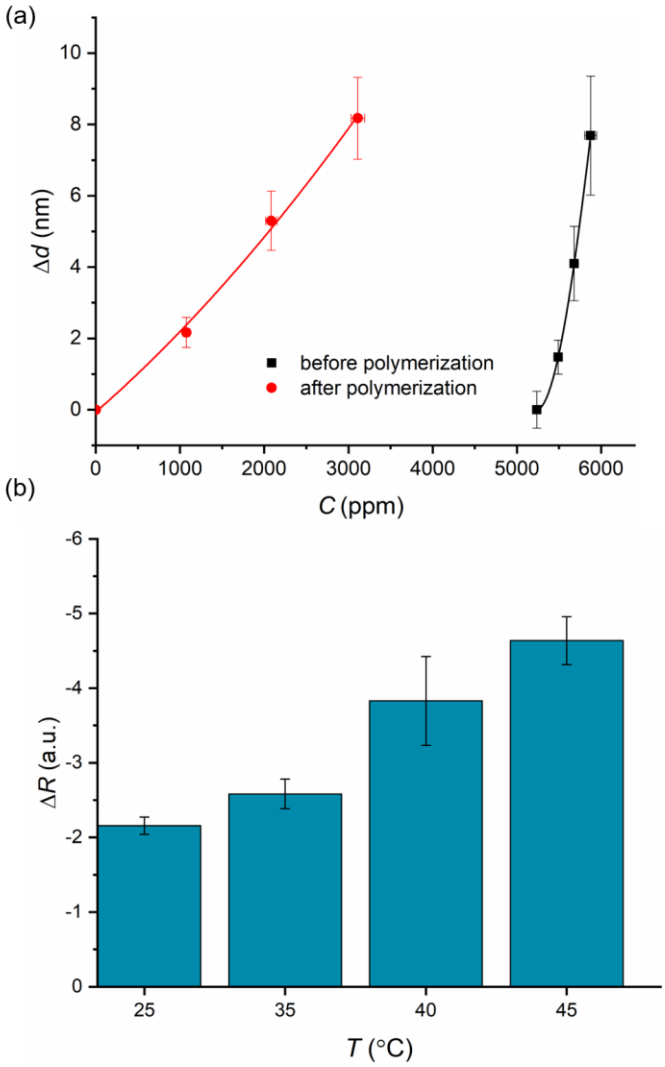

Figure 6. (a) Change in lattice spacing (Δd) of BPII as a function of toluene vapor concentration at 25 °C, before and after polymerization (i.e., with a PSBP) of the BPII. (b) Response of PSBP to toluene vapor concentration of 400 ± 60 ppm at temperatures T = 25, 35, 40, 45°C and atmospheric pressure. Data are based on three independent samples. Error bars are standard deviations.

with toluene concentration over a broad range of concentrations (Figure 6a). Consistent with the results of a prior study,[36] we also found that the lattice spacing of BPII, prior to polymerization, increased with concentration of toluene, although with important differences such as the range of toluene concentration over which a structural response is observed (Figure 6a). Past studies have reported that an increase in temperature leads to an increase in the lattice spacing of BPII, in a

manner that is similar to exposure to toluene.[34, 44, 51] The close correspondence between the effects of toluene and temperature on the structure of BPII hints that the two variables influence the free energy of BPII in similar ways. This conclusion is reinforced by our own measurements (Figure S6, SI) in which we quantified the correspondence between a change in toluene concentration and a change in temperature on phase transitions of the BP mixtures (not polymerized) used in our current study. Below we use this correspondence to provide insight into how both toluene and temperature impact the change in lattice spacing of BPII.

We explored the free energy density of BPII by using a modification of a previously reported theory[47, 52] in which the elastic free energy per unit length of a DTC is expressed as[47]

$$f_{\mathrm{DTC}} = \pi K_{22} \int_0^{q_0\delta} \frac{1}{q_0 r} \sin^2(q_0 r)\mathrm{d}(q_0 r) - \pi(K_{22} + K_{24})\sin^2(q_0\delta) \quad (2)$$

where $q_0 = 2\pi/P$ is called the chirality, P is the pitch, δ is the radius of the DTC, and K_{22} and K_{24} are elastic constants for twist and saddle-splay strains, respectively. Here we assume $K_{24} = 0.5K_{22} = 0.5K$.[47] The temperature-dependence of the elastic constant K is described as being proportional to $(T_{\mathrm{iso}} - T)^{\beta}$, where β is a constant typically ranging from 0.34 to 0.44.[53] The free energy per unit length of disclination located between the DTCs is expressed as[31]

$$f_{\mathrm{defect}} = \frac{1}{4} B\pi K \ln(\delta_{\mathrm{max}}/\delta_{\mathrm{c}}) + a\pi{\delta_{\mathrm{c}}}^2(T_{\mathrm{iso}} - T) + 2\sigma\pi\delta_{\mathrm{c}} \quad (3)$$

where δ_{c} is the radius of the core of the disclination, δ_{max} is a cutoff radius[47] (characteristic radius of the strained volume of material between DTCs), B[54] is a numerical factor that corrects for the assumed cylindrical geometry[1] (see SI for detail), a is the free energy cost per unit volume associated with formation of the disclination core (estimated from the latent heat of the BP-to-isotropic transition) from the bulk LC, and σ is the interfacial tension between the disclination and LC. Specifically, the first term in f_{defect} represents the elastic energy (f_{elastic}) associated with straining of LC in the region between the DTCs and disclination core while the final two terms represent the energies of the disclination core and its interface ($f_{\mathrm{disclination}}$). By assuming that the total length of DTCs and disclinations in a single unit cell of BPII are l_{DTC} and l_{defect}, respectively, we expressed the free energy density of the BPII as $f_{\mathrm{total}} = (l_{\mathrm{DTC}}f_{\mathrm{DTC}} + l_{\mathrm{defec}}f_{\mathrm{defect}})/d^3$, where d is the lattice spacing. With the above-described free energy equation, we sought to understand why the lattice spacing of BPII increases with temperature and toluene concentration.

We first show the calculated relationship between lattice spacing and temperature/toluene concentration (Figure 7a) predicted by our model of BPII. We note that parameter values ($a = 4.5 \times 10^3$ J m^{-3} K, $\sigma = 1\times 10^{-5}$ N m^{-1}) used to make these predictions are similar to those previously reported.[30, 55] Inspection of Figure 7a for BPII (not polymerized) reveals that the lattice spacing of BPII is predicted by the theory to increase with temperature/toluene concentration, which is qualitatively consistent with our experimental observations (Figure 6). To provide insight into the origin of this prediction, we calculated the effect of temperature/toluene concentration on the free energy density of BPII with a fixed lattice spacing. Inspection of Figure 7b reveals that the predicted free energy density of the DTCs increases with temperature/toluene concentration (i.e., less favorable contribution to the free energy of the BP), reflecting the decrease in the magnitude of the elastic constant. In contrast, the energetic penalties associated with elastic strain of the LC

around the disclination core ($f_{elastic}$), and the formation of the disclination core ($f_{disclination}$, core energy plus interfacial energy) both decrease with increasing temperature/toluene concentration. Overall, this analysis reveals that the change in lattice spacing of the BPII induced by temperature/toluene concentration reflects a delicate balance of opposing contributions to the free energy of the BPII film. The observed increase in lattice spacing with temperature/toluene concentration, however, ultimately reflects the dominant effect on the elastic energy of the DTC.

The model reported above was developed for BPII prior to polymerization. Three experimental observations reported in our manuscript support the conclusion that the optical response and lattice spacing change reported in our study is controlled by the elastic energy of the LC and is not a consequence of polymer-induced swelling of the PSBP. First, if the polymer promoted swelling of the BSBP by toluene, the change in lattice spacing of the PSBP would be predicted to be greater than the BP; our experimental observations are opposite to this prediction (see Figure 6). Second, our previous study of BPs[36] revealed that the BPI lattice spacing decreases whereas BPII lattice spacing increases upon exposure to toluene. The opposing behaviors of BPI and BPII are inconsistent with a simple "swelling" of the BP phase underlying the response to toluene. Third, as reported in Figure 4, the optical response that we measure arises from Bragg diffraction from the BP; in the absence of the BP within the RM257 network, we do not measure a significant optical response (even if the RM257 network swells under these conditions).

In our model, we considered the polymer network to change the free energy of the BP via two physical mechanisms. First, we assumed that the presence of the polymer in the core of the defect decreased the volume of the core occupied by mesogens. We defined the fraction of the disclination core volume occupied by polymer to be α (equal to the square of the ratio of the polymer radius and the core radius). Second, we assumed that polymerization influenced the temperature-dependence of the elastic constant of the LC. Past studies have revealed that polymer fibrils formed within LCs influence the ordering of mesogenic molecules near the polymer, inhibiting molecular reorientation in response to external fields or changes in temperature.[56-57] Guided by the observation that the elastic constant K is proportional to the square of the scalar order parameter,[58] we hypothesized that the temperature dependence of K decreased after polymerization (see detail in SI). The associated predictions of our model for the polymerized BPII are shown in Figure 7a. Figure 7a compares the temperature/toluene-dependence of the lattice spacing of polymerized BPII (α = 0.65) to the BPII prior to polymerization. Consistent with the experimental measurements in Figure 6a, the rate of change of the lattice spacing with respect to toluene concentration for polymerized BPII is lower than that for the BPII prior to polymerization. Selection of a different value of α does not change this qualitative conclusion (Figure S7, SI), and thus we interpret our model to suggest that a key effect of the polymer network on the response of the PSBP to temperature/toluene concentration is via the impact of the polymer network on K. In addition, inspection of Figure 7a reveals that the lattice spacing is more sensitive to temperature/toluene concentration at higher temperatures. This result leads to the prediction that a larger response to toluene will occur at an elevated temperature, a prediction that is supported by our experimental observations shown in Figure 6b.

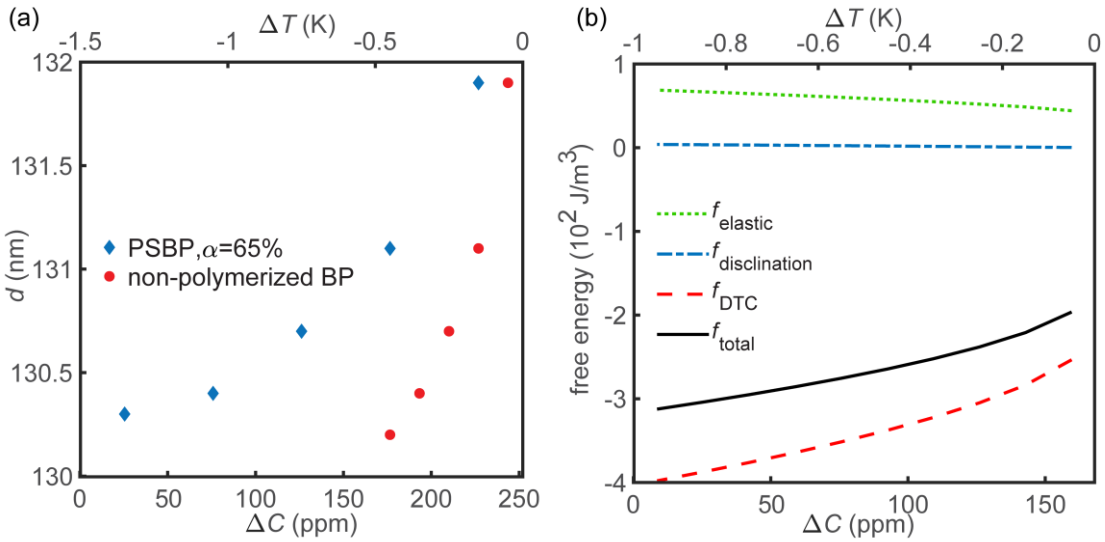

Figure 7. (a) Calculated temperature or toluene vapor concentration-dependence of the lattice spacing of a PSBP (blue symbols) or non-polymerized BPII (brown symbols). We note that $\Delta T = 0$ or $\Delta C = 252$ ppm coincides with formation of an isotropic phase. (b) Calculated temperature or toluene vapor concentration-dependence of the three components of the free energy density at a fixed lattice spacing: DTCs (red line), disclinations (blue line), and elastic energy surrounding the disclinations (green line). The total free energy density is shown by the black line.

The predictions of our model closely align with our experimental findings, and provide insight into the origin of the optical response of PSBP to toluene vapor. However, our results also generate additional questions that deserve future investigation. First, we do not yet fully understand how toluene is distributed within the PSBP film and, specifically, whether or not it is localized in the disclinations. Similarly, we do not yet know how differences in the structure of the polymer networks formed in the nematic, cholesteric and BP impact the response of the polymerized LCs to toluene vapor. Second, our study focused on polymerization in BPII. However, BPI can also be polymerized, and the model that we used to describe the free energy of BPII suggests that the response of polymerized BPI to toluene vapor will differ significantly from BPII (as the volume between the DTCs and disclinations is larger for BPI than BPII).[59] Third, an opportunity exists to develop more detailed models of the free energy of the LC strained between the DTCs and disclinations. In particular, the simplifying assumption of a cylindrical geometry should be addressed in a future model. Finally, we do not yet have a full understanding of why the toluene-triggered change in reflectivity of the polymerized cholesteric films is opposite in sign to the polymerized nematic and BPs.

In addition to the fundamental issues mentioned above, we wish to also comment on several points related to the potential application of PSBP as a wearable sensor. First, our study does not address the selectivity of the response of the PSBP to toluene relative to other VOCs. We note, however, that there are applications of sensors for VOCs where the identity of the analyte is known and selectivity to a particular VOC is not essential, such as identifying the extent of

exposure of workers to VOCs in industrial painting facilities. In addition, a past study has revealed that BPs (not polymerized) do exhibit a selectivity towards aromatic compounds (toluene, styrene…) relative to other VOCs such as ethanol, dichloromethane, acetonitrile.[36] For example, to achieve the same optical response from a BP, the vapor concentration of acetonitrile was 9.3 times higher than toluene.[36] Second, we comment that the intensity of light reflected from a PSBP will depend on the viewing angle. Thus, in any quantitative PSBP-based sensing device, it will be necessary to fix the viewing angle, as can be achieved by using, for example, a smart phone camera or by integrating a light source and a detector into a miniature cell with a fixed optical path.[61-62]

Conclusion

In summary, this study characterizes the influence of polymerization on the structural and optical response of BPs to toluene vapor. We found that PSBPs, which have been shown to possess mechanical properties that enable their integration into devices, also exhibit an optical response to toluene vapor over a broad range of concentrations (140 ± 10 ppm to ~ 5155 ± 60 ppm) and temperatures (25 °C to 45 °C). We established that the response arises from toluene-induced changes in the lattice spacing of the PSBP, resulting in a shift in the Bragg reflection intensity. We also compared the toluene-induced response of the PSBP to polymerized cholesteric and polymerized nematic phases, and found the sensitivity of the PSBP to be six-fold higher than either the polymerized cholesteric or polymerized nematic phases. The dynamics of the response of the polymerized chiral phases were measured to be twice as fast as the achiral nematic phase, supporting our conclusion that the effect of toluene on the chiral supramolecular structure (DTC and thus lattice spacing) of the PSBP underlies its responsiveness. This conclusion is further supported by predictions of a simple thermodynamic theory of the equilibrium structure of PSBPs, which highlighted the dominant effect of toluene on the energetics of DTCs within the BPs.

Overall, we conclude that polymerized BPs offer the basis of promising materials for passive reporting of VOCs. The limit of detection (140 ± 10 ppm at 25 °C) to toluene vapor that we measured is relevant to human exposure limits established by OSHA (200 ppm time-averaged over 8-hours). We note also that the mechanism underlying the response of PSBPs to VOCs (lattice spacing change) is likely applicable to detection of other molecules that lack chemical reactivity (e.g., polychlorinated biphenyls in water pollution[60]). Additionally, the formation of the polymer-stabilized BP can be viewed as introducing a guest (i.e., polymer) into the defects of the BP. The presence of the guest not only stabilizes the BP, but also introduces the future possibility of programming interactions between targeted molecular species (stimulus) and guest components in the LC to achieve high levels of selectivity.[63-64] Finally, PSBPs have been widely investigated as promising optical or electro-optical elements,[65-66] and our study points towards the possibility of incorporating chemoresponsive functionalities into photonic devices based on the polymerized thin LC films.

ASSOCIATED CONTENT

Supporting Information Schematic illustration of exposure system; Optical micrographs of PSBP and BP (not polymerized) at different temperatures; Kossel diagram technique; Optical response of PSBP to toluene vapor at concentrations lower than 1000 ppm; Reflectance spectrum for PSBP at 25 ℃; Reflectance spectrum of the non-polymerized BP as a function of toluene

concentrations at 25 °C; Mapping between temperature and toluene concentration; Free energy model calculation. (PDF) The following file is available free of charge.

AUTHOR INFORMATION

Corresponding Author

* E-mail: nabbott@cornell.edu (Nicholas L. Abbott)

Present Addresses

†Department of Chemical Engineering, Pohang University of Science and Technology, 77 Cheongam-Ro, Nam-Gu, Pohang, Gyengbuk, 37673 Korea

Author Contributions

The manuscript was written through contributions of all authors. All authors have given approval to the final version of the manuscript.

Funding Sources

The experiments reported in this paper were supported by the Army Research Office (W911NF-15-1-0568 and W911NF-19-1-0071) and National Science Foundation (CBET-1803409 and CBET-1852379). The calculations were supported by the Department of Energy, Basic Energy Sciences, Division of Materials Research, Biomaterials Program under Grant No. DE-SC0019762. This work made use of the Cornell Center for Materials Research Shared Facilities which are supported through the NSF MRSEC program (DMR-1719875). Support of the Department of Chemical and Biological Engineering at University of Wisconsin-Madison (partial stipend for YY) is acknowledged.

Notes

Nicholas Abbott is a co-founder of Platypus Technologies LLC, a for-profit company that has commercialized liquid crystal-based analytical technologies.

References

(1) de Gennes, P. G.; Prost, J. *The Physics of Liquid Crystals*, Oxford University Press Inc.: New York, 1993.

(2) Jerome, B. Surface Effects and Anchoring in Liquid Crystals. *Rep. Prog. Phys.* **1991**, *54* (3), 391-451.

(3) Schiekel, M. F.; Fahrenschon, K. Deformation of Nematic Liquid Crystals with Vertical Orientation in Electrical Fields. *Appl. Phys. Lett.* **1971**, *19* (10), 391-393.

(4) Schadt, M.; Helfrich, W. Voltage-dependent Optical Activity of a Twisted Nematic Liquid Crystal. *Appl. Phys. Lett.* **1971**, *18* (4), 127-128.

(5) Ireland, P. T.; Jones, T. V. Liquid Crystal Measurements of Heat Transfer and Surface Shear Stress. *Meas. Sci. Technol.* **2000**, *11* (7), 969-986.

(6) Nayani, K.; Rai, P.; Bao, N.; Yu, H.; Mavrikakis, M.; Twieg, R. J.; Abbott, N. L. Liquid Crystals with Interfacial Ordering that Enhances Responsiveness to Chemical Targets. *Adv. Mater.* **2018**, *30* (27), 1706707.

(7) Shah, R. R.; Abbott, N. L. Principles for Measurement of Chemical Exposure Based on Recognition-Driven Anchoring Transitions in Liquid Crystals. *Science* **2001**, *293* (5533), 1296-1299.

(8) Yu, H.; Szilvási, T.; Rai, P.; Twieg, R. J.; Mavrikakis, M.; Abbott, N. L. Computational Chemistry-Guided Design of Selective Chemoresponsive Liquid Crystals Using Pyridine and Pyrimidine Functional Groups. *Adv. Funct. Mater.* **2018**, *28* (13), 1703581.

(9) Shah, R. R.; Abbott, N. L. Orientational Transitions of Liquid Crystals Driven by Binding of Organoamines to Carboxylic Acids Presented at Surfaces with Nanometer-Scale Topography. *Langmuir* **2003**, *19* (2), 275-284.

(10) Brake, J. M.; Daschner, M. K.; Luk, Y.-Y.; Abbott, N. L. Biomolecular Interactions at Phospholipid-decorated Surfaces of Liquid Crystals. *Science* **2003**, *302* (5653), 2094-2097.

(11) Macri, K. M.; Noonan, P. S.; Schwartz, D. K. Receptor-Mediated Liposome Fusion Kinetics at Aqueous/Liquid Crystal Interfaces. *ACS Appl. Mater. Interfaces* **2015**, *7* (36), 20400-20409.

(12) Lai, S. L.; Tan, W. L.; Yang, K-L. Detection of DNA Targets Hybridized to Solid Surfaces Using Optical Images of Liquid Crystals. *ACS Appl. Mater. Interfaces* **2011**, *3* (9), 3389-3395.

(13) Bedolla Pantoja, M. A.; Abbott, N. L. Surface-Controlled Orientational Transitions in Elastically Strained Films of Liquid Crystal That Are Triggered by Vapors of Toluene. *ACS Appl. Mater. Interfaces* **2016**, *8* (20), 13114-13122.

(14) Kieser, B.; Pauluth, D.; Gauglitz, G. Nematic Liquid Crystals as Sensitive Layers for Surface Plasmon Resonance Sensors. *Anal. Chim. Acta* **2001**, *434* (2), 231-237.

(15) Drapp, B.; Pauluth, D.; Krause, J.; Gauglitz, G. The Application of the Phase Transition in Nematic Liquid Crystals for the Optical Detection of Volatile Organic Compounds. *Fresenius' J. Anal. Chem.* **1999**, *364* (1), 121-127.

(16) Mujahid, A.; Stathopulos, H.; Lieberzeit, P. A.; Dickert, F. L. Solvent Vapour Detection with Cholesteric Liquid Crystals—Optical and Mass-Sensitive Evaluation of the Sensor Mechanism. *Sensors* **2010**, *10* (5), 4887-4897.

(17) Chang, C.-K.; Kuo, H.-L.; Tang, K.-T.; Chiu, S.-W. Optical Detection of Organic Vapors Using Cholesteric Liquid Crystals. *Appl. Phys. Lett.* **2011**, *99* (7), 073504.

(18) Winterbottom, D. A.; Narayanaswamy, R.; Raimundo Jr, I. M. Cholesteric Liquid Crystals for Detection of Organic Vapours. *Sens. Actuators B Chem.* **2003**, *90* (1–3), 52-57.

(19) Mulder, D. J.; Schenning, A. P. H. J.; Bastiaansen, C. W. M. Chiral-nematic Liquid Crystals as One Dimensional Photonic Materials in Optical Sensors. *J. Mater. Chem. C* **2014**, *2* (33), 6695-6705.

(20) Lai, Y.-T.; Kuo, J.-C.; Yang, Y.-J. A Novel Gas Sensor Using Polymer-Dispersed Liquid Crystal Doped with Carbon Nanotubes. *Sens. Actuators, A* **2014**, *215*, 83-88.

(21) U.S. EPA. EPA's Report on the Environment (ROE) (2008 Final Report). U.S. Environmental Protection Agency, Washington, D.C., EPA/600/R-07/045F (NTIS PB2008-112484), 2008.

(22) OSHA InfoSheet: Toluene Safety in the Workplace. U.S. Department of Labor, Occupational Health & Safety Administration: Washington, DC., 2013.

(23) Zhang, Y.; Zhang, M.; Cai, Z. Q.; Chen, M. Q.; Cheng, F. L. A Novel Electrochemical Sensor for Formaldehyde based on Palladium Nanowire Arrays Electrode in Alkaline Media. *Electrochim. Acta* **2012**, *68*, 172-177.

(24) Heglund, D. L.; Tilotta, D. C. Determination of Volatile Organic Compounds in Water by Solid Phase Microextraction and Infrared Spectroscopy. *Environ. Sci. Technol.* **1996**, *30* (4), 1212-1219.

(25) Mirzaei, A.; Leonardi, S. G.; Neri, G. Detection of Hazardous Volatile Organic Compounds (VOCs) by Metal Oxide Nanostructures-Based Gas Sensors: A Review. *Ceram. Int.* **2016**, *42* (14), 15119-15141.

(26) Lee, H.-G.; Munir, S.; Park, S.-Y. Cholesteric Liquid Crystal Droplets for Biosensors. *ACS Appl. Mater. Interfaces* **2016**, *8* (39), 26407-26417.

(27) Ryabchun, A.; Yakovlev, D.; Bobrovsky, A.; Katsonis, N. Dynamic Diffractive Patterns in Helix-Inverting Cholesteric Liquid Crystals. *ACS Appl. Mater. Interfaces* **2019**, *11* (11), 10895-10904.

(28) Kikuchi, H. Liquid Crystalline Blue Phases. In *Liquid Crystalline Functional Assemblies and Their Supramolecular Structures*; Kato, T., Ed.; Springer Berlin Heidelberg: 2008; pp 99-117.

(29) Wright, D. C.; Mermin, N. D. Crystalline Liquids: the Blue Phases. *Rev. Mod. Phys.* **1989**, *61* (2), 385-432.

(30) Meiboom, S.; Sammon, M.; Brinkman, W. F. Lattice of Disclinations: The Structure of The Blue Phases of Cholesteric Liquid Crystals. *Phys. Rev. A* **1983**, *27* (1), 438-454.

(31) Meiboom, S.; Sethna, J. P.; Anderson, P. W.; Brinkman, W. F. Theory of the Blue Phase of Cholesteric Liquid Crystals. *Phys. Rev. Lett.* **1981**, *46* (18), 1216-1219.

(32) Bukusoglu, E.; Wang, X.; Martinez-Gonzalez, J. A.; de Pablo, J. J.; Abbott, N. L. Stimuli-Responsive Cubosomes Formed from Blue Phase Liquid Crystals. *Adv. Mater.* **2015**, *27* (43), 6892-6898.

(33) Kikuchi, H.; Yokota, M.; Hisakado, Y.; Yang, H.; Kajiyama, T. Polymer-stabilized Liquid Crystal Blue Phases. *Nat. Mater.* **2002**, *1* (1), 64-68.

(34) Coles, H. J.; Pivnenko, M. N. Liquid Crystal 'Blue Phases' with a Wide Temperature Range. *Nature* **2005**, *436* (7053), 997-1000.

(35) Castles, F.; Morris, S. M.; Hung, J. M.; Qasim, M. M.; Wright, A. D.; Nosheen, S.; Choi, S. S.; Outram, B. I.; Elston, S. J.; Burgess, C.; Hill, L.; Wilkinson, T. D.; Coles, H. J. Stretchable Liquid-crystal Blue-phase Gels. *Nat. Mater.* 2014, *13* (8), 817-821.

(36) Bedolla Pantoja, M. A.; Yang, Y.; Abbott, N. L. Toluene-induced Phase Transitions in Blue Phase Liquid Crystals. *Liq. Cryst.* **2019**, *46* (13-14), 1925-1936.

(37) Jo, S.-Y.; Jeon, S.-W.; Kim, B.-C.; Bae, J.-H.; Araoka, F.; Choi, S.-W. Polymer Stabilization of Liquid-Crystal Blue Phase II toward Photonic Crystals. *ACS Appl. Mater. Interfaces* **2017**, *9* (10), 8941-8947.

(38) Yoshida, H.; Tanaka, Y.; Kawamoto, K.; Kubo, H.; Tsuda, T.; Fujii, A.; Kuwabata, S.; Kikuchi, H.; Ozaki, M. Nanoparticle-Stabilized Cholesteric Blue Phases. *Appl. Phys. Express* **2009**, *2* (12), 121501.

(39) Karatairi, E.; Rozic, B.; Kutnjak, Z.; Tzitzios, V.; Nounesis, G.; Cordoyiannis, G.; Thoen, J.; Glorieux, C.; Kralj, S. Nanoparticle-induced Widening of the Temperature Range of Liquid-crystalline Blue Phases. *Phys. Rev. E* **2010**, *81* (4), 041703.

(40) Park, K.-W.; Gim, M.-J.; Kim, S.; Hur, S.-T.; Choi, S.-W. Liquid-Crystalline Blue Phase II System Comprising a Bent-Core Molecule with a Wide Stable Temperature Range. *ACS Appl. Mater. Interfaces* **2013**, *5* (16), 8025-8029.

(41) Yokoyama, S.; Mashiko, S.; Kikuchi, H.; Uchida, K.; Nagamura, T. Laser Emission from a Polymer-Stabilized Liquid-Crystalline Blue Phase. *Adv. Mater.* **2006**, *18* (1), 48-51.

(42) Lin, J.-D.; Wang, T.-Y.; Mo, T.-S.; Huang, S.-Y.; Lee, C.-R. Wide-Band Spatially Tunable Photonic Bandgap in Visible Spectral Range and Laser based on a Polymer Stabilized Blue Phase. *Sci Rep* **2016**, *6* (1), 30407.

(43) Li, X.; Martínez-González, J. A.; Park, K.; Yu, C.; Zhou, Y.; de Pablo, J. J.; Nealey, P. F. Perfection in Nucleation and Growth of Blue-Phase Single Crystals: Small Free-Energy Required to Self-Assemble at Specific Lattice Orientation. *ACS Appl. Mater. Interfaces* **2019**, *11* (9), 9487-9495

(44) Du, X.-W.; Hou, D.-S.; Li, X.; Sun, D.-P.; Lan, J.-F.; Zhu, J.-L.; Ye, W.-J. Symmetric Continuously Tunable Photonic Band Gaps in Blue-Phase Liquid Crystals Switched by an Alternating Current Field. *ACS Appl. Mater. Interfaces* **2019**, *11* (24), 22015-22020.

(45) Kamal, T.; Park, S.-Y. Shape-Responsive Actuator from a Single Layer of a Liquid-Crystal Polymer. *ACS Appl. Mater. Interfaces* **2014**, *6* (20), 18048-18054.

(46) Rajaram, C. V.; Hudson, S. D.; Chien, L. C. Morphology of Polymer-Stabilized Liquid Crystals. *Chem. Mater.* **1995**, *7* (12), 2300-2308.

(47) Yang, D.-K.; Wu, S.-T. Blue Phases of Chiral Liquid Crystals. In *Fundamentals of liquid crystal devices*, John Wiley & Sons: 2014.

(48) Bukusoglu, E.; Martinez-Gonzalez, J. A.; Wang, X.; Zhou, Y.; de Pablo, J. J.; Abbott, N. L. Strain-induced Alignment and Phase Behavior of Blue Phase Liquid Crystals Confined to Thin Films. *Soft Matter* **2017**, *13* (47), 8999-9006.

(49) Chen, C.-W.; Hou, C.-T.; Li, C.-C.; Jau, H.-C.; Wang, C.-T.; Hong, C.-L.; Guo, D.-Y.; Wang, C.-Y.; Chiang, S.-P.; Bunning, T. J.; Khoo, I.-C.; Lin, T.-H. Large Three-dimensional Photonic Crystals Based on Monocrystalline Liquid Crystal Blue Phases. *Nat Commun* **2017**, *8* (1), 727.

(50) Chen, G.-H.; Springer, J. Sorption and Diffusion of Gases in Liquid Crystalline Substances. *Mol. Cryst. Liq. Cryst. Sci. Technol., Sect. A* **2000**, *339* (1), 31-44.

(51) Choi, H.; Higuchi, H.; Kikuchi, H. Fast Electro-optic Switching in Liquid Crystal Blue Phase II. *Appl. Phys. Lett.* **2011**, *98* (13), 131905.

(52) Fukuda, J.-i. Stabilization of Blue Phases by the Variation of Elastic Constants. *Phys. Rev. E* **2012**, *85* (2), 020701.

(53) Haller, I. Thermodynamic and Static Properties of Liquid Crystals. *Prog. Solid State Chem.* **1975**, *10*, 103-118.

(54) Castles, F.; Morris, S. M.; Terentjev, E. M.; Coles, H. J. Thermodynamically Stable Blue Phases. *Phys. Rev. Lett.* **2010**, *104* (15), 157801.

(55) Fukuda, J.-i. Stabilization of a Blue Phase by a Guest Component: An Approach Based on a Landau-de Gennes Theory. *Phys. Rev. E* **2010**, *82* (6), 061702.

(56) Chiccoli, C.; Pasini, P.; Skačej, G.; Zannoni, C.; Žumer, S. Polymer Network-induced Ordering in a Nematogenic Liquid: A Monte Carlo Study. *Phys. Rev. E* **2002**, *65* (5), 051703.

(57) Yang, D.-K.; Cui, Y.; Nemati, H.; Zhou, X.; Moheghi, A. Modeling Aligning Effect of Polymer Network in Polymer Stabilized Nematic Liquid Crystals. *J. Appl. Phys.* **2013**, *114* (24), 243515.

(58) Maier, W.; Saupe, A. Eine einfache molekular-statistische Theorie der nematischen kristallinflüssigen Phase. Teil II. *Z. Naturforsch. A* **1960**, *15* (4), 287-292.

(59) Miller, R. J.; Gleeson, H. F. Lattice Parameter Measurements from the Kossel Diagrams of the Cubic Liquid Crystal Blue Phases. *J. Phys. II France* **1996**, *6* (6), 909-922.

(60) Yu, Y.; Chen, X.; Wei, Y.; Liu, J.-H.; Huang, X.-J. Strategy for Polychlorinated Biphenyl Detection Based on Specific Inhibition of Charge Transport Using a Nanogapped Gold Particle Film. *Anal. Chem.* **2012**, *84* (22), 9818-9824.

(61) Nandi, R.; Pal, S. K. Liquid Crystal Based Sensing Device Using a Smartphone. *Analyst* **2018**, *143* (5), 1046-1052.

(62) Jun, L.; Qiulin, T.; Wendong, Z.; Chenyang, X.; Tao, G.; Jijun, X. Miniature Low-power IR Monitor for Methane Detection. *Measurement* **2011**, *44* (5), 823-831.

(63) Han, Y.; Pacheco, K.; Bastiaansen, C. W. M.; Broer, D. J.; Sijbesma, R. P. Optical Monitoring of Gases with Cholesteric Liquid Crystals. *J. Am. Chem. Soc.* **2010**, *132* (9), 2961-2967.

(64) Sutarlie, L.; Lim, J. Y.; Yang, K.-L. Cholesteric Liquid Crystals Doped with Dodecylamine for Detecting Aldehyde Vapors. *Anal. Chem.* **2011**, *83* (13), 5253-5258.

(65) Yang, J.; Zhao, W.; Yang, Z.; He, W.; Wang, J.; Ikeda, T.; Jiang L. Photonic Shape Memory Polymer Based on Liquid Crystalline Blue Phase Films. *ACS Appl. Mater. Interfaces* **2019**, *11* (49), 46124-46131.

(66) Sridurai, V.; Mathews, M.; Yelamaggad, C. V.; Nair, G. G. Electrically Tunable Soft Photonic Gel Formed by Blue Phase Liquid Crystal for Switchable Color-Reflecting Mirror. *ACS Appl. Mater. Interfaces* **2017**, *9* (45), 39569-39575.

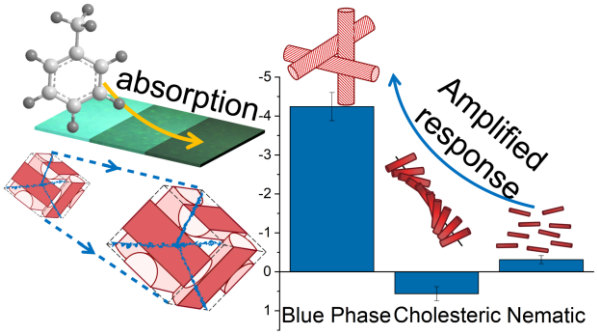

Abstract Graphic